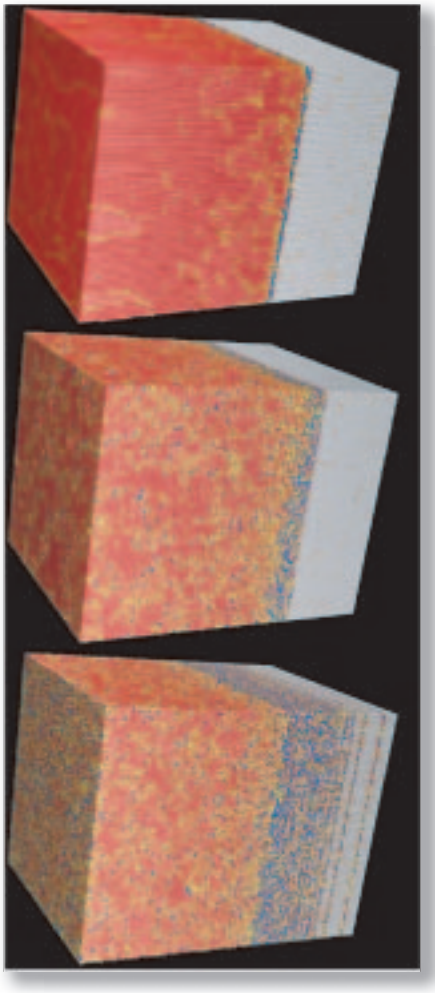

**Figure 1. Orientation dependence of the shock-induced bcc → hcp polymorphic phase transformation in iron. Samples contain ~ 8 million atoms (40 nm x 40 nm x 57nm), and are shown 6.57 ps after impact with a piston traveling at velocity $u_p$ = 1087 m/s. From top to bottom, samples are shocked in the bcc [001], [011], and [111] directions. Atoms are color-coded by the number of neighbors n within 2.75 Å: the unshocked bcc lattice (n = 8) is gray, uniaxially compressed bcc (n = 10) is blue, and the transformed close-packed grains (n = 12) are red, separated by yellow (n = 11) grain boundaries.**

# Investigating the Mechanical Deformation of Metals Using Large-Scale Molecular Dynamics Simulations

**Timothy C. Germann (X-7), James E. Hammerberg (X-7), Brad Lee Holian (T-12), Kai Kadau (T-11), Peter S. Lomdahl (T-11), and Ramon Ravelo (X-7 & UTEP)**

**ASC Materials Modeling Project Leader: Frank Addessio (T-3)**
**ASC Materials and Physics Models Program Manager: Paul Dotson (T-DO)**

Large-scale nonequilibrium molecular dynamics (NEMD) simulations of metals subjected to high-strain rate loading (compression and/or shear) provide a unique insight into the fundamental mechanisms behind shock-induced plasticity, phase transformations, tensile failure, and sliding friction. In the context of the ASC Materials and Physics Models (M&PM) development efforts, they provide a crucial bridge between *ab initio* electronic structure calculations of the interactions between individual atoms, and the mesoscopic dynamics of discrete dislocations or phase-fields. Modern computational facilities, including the ASC Q machine, its unclassified counterpart (QSC), and the M&PM Beowulf cluster (Grendels), have been used to simulate the 3-D dynamics of up to 100 million atoms, for timescales from tens to hundreds of picoseconds. Three examples that will be highlighted here are the alpha-to-epsilon phase transformation of solid iron under shock compression, material failure (including ejection) upon shock release, and interfacial sliding friction between dissimilar metals.

## Shock-Induced Solid-Solid Phase Transformations

The orientation-dependent shock response of individual grains making up a bulk polycrystalline sample is a prime example of a problem requiring large-scale NEMD simulations; studying a single unit cell (or even a small number of unit cells) does not allow the collective long-range rearrangements by which metals deform. Shown in Figure 1 are three simulations of iron single crystals, shocked to the same particle velocity $u_p$ and shown at the same time after impact; the only difference is the crystallographic direction in which shock compression takes place. In addition to the expected anisotropic shock velocities (related to the anisotropic sound speeds), significant differences in the phase transformation timescale, and the subgrain size of the resulting product phase, are evident; large twins are created by [001] compression[1], whereas crystallites are barely visible in the [111] case.

This work has spawned interest among our experimental colleagues in DX-, P- and C-Divisions, and external collaborators at UCSD, Oxford, and LLNL. An LDRD-DR, "*Probing the Structural Dynamics of Condensed Matter with Ultrafast X-ray Diffraction*," began in FY02 with the express goal of tracking the dynamic phase changes in laser-shocked, oriented single crystal Fe and/or Ga targets.

**Tensile Failure Following Shock Release**

We have also probed various aspects of the shock unloading process using large-scale NEMD simulations. Shown in Figure 2 is an example of the atomistic ejecta spray and nanojetting that occurs when a planar shock wave (top frame) encounters a grooved free Cu surface. The sample here contains 3 million atoms in a thin slab geometry (3 nm x 72 nm x 276 nm), with a 26.6° groove. For the case of a perfectly smooth surface, we have measured the ejecta particle size and velocity distributions, as well as the total areal density, as functions of shock strength (through the melt transition), necessary input for the development of advanced ejecta source models. The jetting, illustrated in Figure 2, points out an additional contribution, which will presumably dominate the total ejecta mass for typical machined surfaces: the formation of a nanojet which ultimately breaks up into relatively large ejecta clusters. The breakup times, and hence particle size and velocity distributions, depend strongly on shock strength. This can be seen in the lower frames of Figure 2, where stronger shocks (with higher jet temperatures) lead to earlier jet breakup. Multidivisional efforts are underway to secure LDRD-DR or other funding for the development of advanced imaging diagnostics to track the emission of ejecta particles from perfect and machined metal surfaces, including a tightly integrated NEMD simulation component.

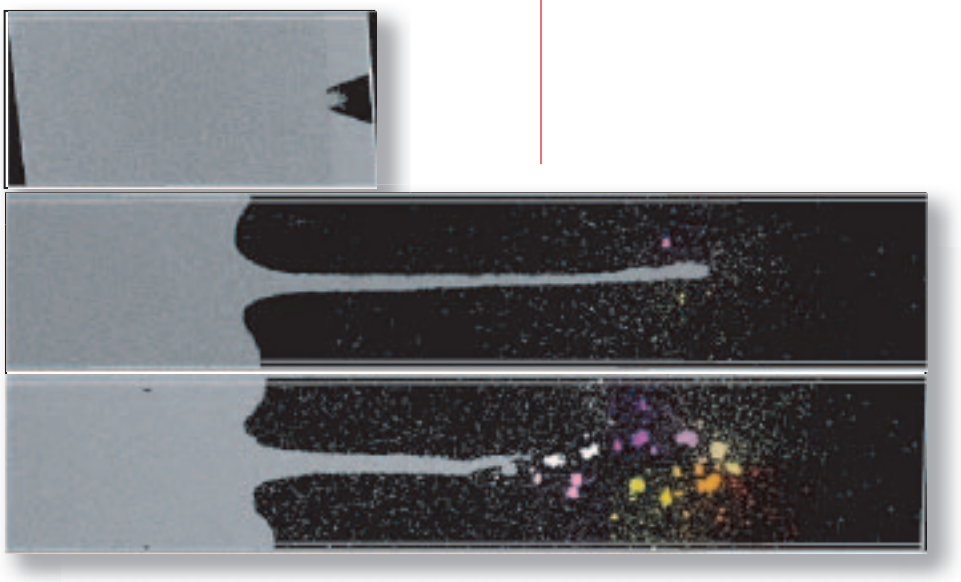

**Figure 2. Ejecta formation in copper when a strong shock wave rebounds from a grooved surface in an otherwise perfect crystal (top frame). In addition to a small amount of atomic ejecta created upon the initial release, the expanding nanojet (middle frame) later becomes unstable and breaks up, creating large ejecta clusters (bottom frame). This breakup occurs sooner the stronger the initial shock (middle frame: particle velocity $u_p$ = 3.3 km/s, 48.6 ps after impact; bottom frame: $u_p$ = 4.3 km/s, 43.2 ps after impact).**

A second important process which occurs upon shock unloading is spallation. Spallation takes place when two release waves collide, rather than the single release wave creating ejecta (in flyer-plate experiments, the second release wave comes from the relatively thin flyer plate). As seen in Figure 1, the shock rise time in perfect single crystals is remarkably short (corresponding to the traversal of only a few lattice planes), so the strain rate in single crystals is exceptionally high compared to bulk, polycrystalline samples where the shock front spreads due to grain anisotropy, wave

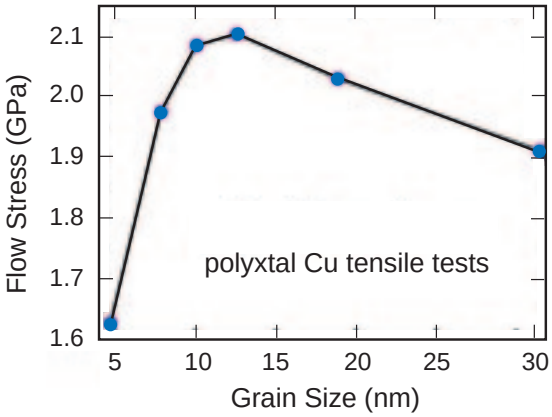


**Figure 3. Transition to normal Hall-Petch behavior in nanocrystalline Cu.**

reflection, and scattering. To contribute to the understanding of spall failure in polycrystalline samples, we have studied the tensile loading of nanocrystalline NEMD samples of fcc metals (Cu, Al, Ni) created in various manners (e.g., annealing conditions). We have observed the crossover in behavior (Figure 3) from strengthening with increasing grain size for grains below ~ 15 nm (presumably due to a grain boundary sliding-dominated response), to the conventional Hall-Petch $d^{-1/2}$ weakening with increasing grain size d for larger samples, where plastic deformation is accomplished primarily via intragrain dislocations. An independent confirmation of these results for Cu has recently been published.[2]

**High-Speed Interfacial Sliding Friction**

NEMD simulations allow one to form a picture of the importance of various micro- and meso-scopic physical processes in thermodynamic regimes that are difficult to examine by means of standard experimental techniques (although new efforts are underway, as mentioned above). This is particularly true for the physics of high-speed dry friction between ductile metals at arbitrary densities. By high speed we mean interfacial velocities of order 1/10 or more of the material sound speed c at the density of interest. Such regimes are encountered in dynamic experiments, where pressures may reach several tens of GPa. Several dynamic experiments at Los Alamos, namely ATLAS and Proton Radiography experiments for high velocities, and DX-3 rotating-barrel gas gun experiments at lower velocities, are providing data for macroscopic models of the tangential force at a ductile metal interface, but the general framework for such a model has been established via extensive 2-D and 3-D NEMD simulations.

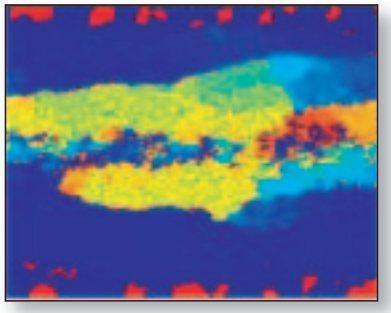

**Figure 4. Molecular dynamics simulation of 2-D Cu/Cu interfacial sliding. Atoms are colored according to the local rotation angle of the hexagonal lattice, from equivalent blue (– 30˚) to red (+ 30˚) configurations.**

The general picture that has emerged from these simulations over the past several years is one of multiple interacting length and time scales, and a dynamic formation of microstructure at the sliding interface in the nonequilibrium steady state (Figure 4). Figure 5 shows NEMD results for the frictional force per unit area for single crystal Al sliding on single crystal Ta, as a function of relative velocity. There are three regimes of particular interest. At low velocities, the frictional force increases roughly linearly with relative velocity, as phonon dissipation and low-dislocation densities dominate the sliding process. At higher relative velocities, around $0.1c_{Al}$, a weakening of the interface occurs. This is associated with a structural transformation in the weaker Al, resulting in a strongly disordered region near the interface that persists into the third, high-velocity, regime where simple arguments from high-rate plasticity and subgrain energetics predict a power-law behavior with exponent – 3/4 shown by the full lines. Figure 6 shows the high-velocity sliding behavior in Cu/Ag, where the differences in hardness are not so marked. A centrosymmetric order parameter is used to distinguish dislocation, stacking fault, and grain boundary atoms. The dislocation loop and stacking fault structure in the stronger Cu workpiece, and the more complex dislocation and near-interface subgrain structure generated during sliding in the weaker Ag, are evident.

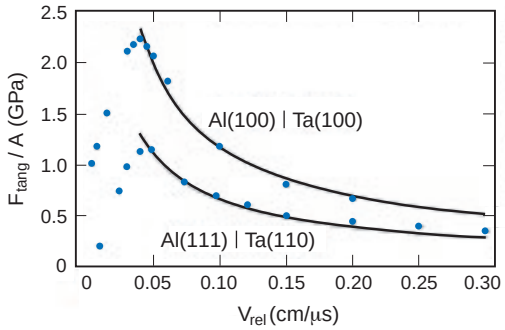


**Figure 5. Frictional force per unit area vs. sliding velocity for two Ta/Al interfaces, with a 15 GPa applied normal pressure. The lower velocity regime is dominated by anharmonic phonon dissipation, and the high-velocity regime (beginning at ~1/10th of the transverse sound speed) is characterized by the formation of a graded nanostructure near the interface and a related $v^{-3/4}$ decrease of the frictional force with velocity (solid lines).**

## Outlook

With the recent development (supported in part by the LANL ASC program) of advanced interatomic potentials for Pu, Ga, and their alloys, we will be able to investigate the rich dynamics of these more complex (partially covalent) metals as they are subjected to shock compression and interfacial sliding. The increasing computational power available in coming years through the ASC program will also enable the routine simulation of polycrystalline samples with grain sizes above the crossover to the "normal Hall-Petch" regime of dislocation-dominated plasticity.

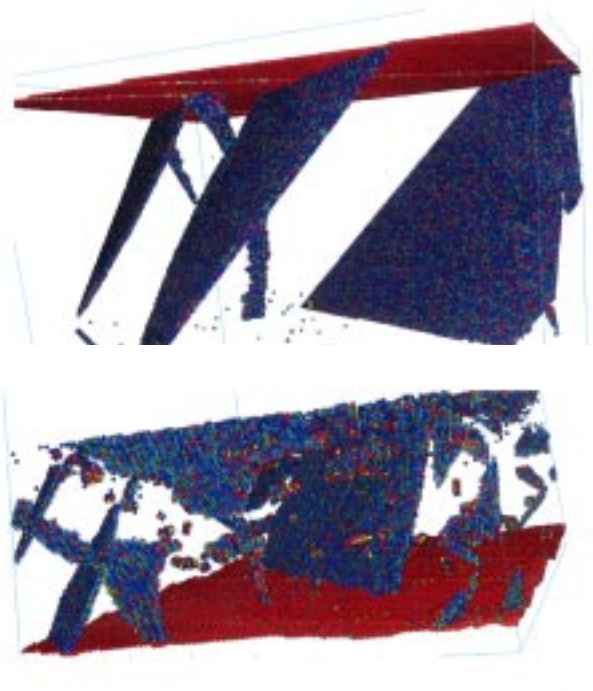

**Figure 6. Dislocation structure produced by Cu/Ag interfacial sliding at 5 GPa normal pressure and $v_{rel}$ = 758 m/s. Atoms in perfect fcc sites are not shown, leaving only surface (red) and dislocation core (mainly blue) atoms. Both planar stacking faults and perfect dislocation loops are evident in the Cu (top) and Ag (bottom) workpieces.**

**We wish to gratefully acknowledge the support from James A. Peery and Kenneth R. Koch.**

[1]K. Kadau, T. C. Germann, P. S. Lomdahl, and B. L. Holian, *Science* **296**, 1681 (2002).

[2]J. Schiøtz and K. W. Jascobsen, *Science* **301**, 1357 (2003).

Contact: Paul J. Dotson
505-667-6107, dotson@lanl.gov

A US Department of Energy Laboratory.

LA-UR-03-7548
T-DO/jshepard

Los Alamos National Laboratory, an affirmative action/equal opportunity employer, is operated by the University of California and the United States Department of Energy under contract W-7405-ENG-36.